

LA-UR-

09-01639

Approved for public release;  
distribution is unlimited.

*Title:* Influence of Carbon Partitioning Kinetics on Final Austenite Fraction during Quenching and Partitioning

*Author(s):* A.J. Clarke, J.G. Speer, D.K. Matlock, F.C. Rizzo, D.V. Edmonds, M.J. Santofimia

*Intended for:* Scripta Materialia



Los Alamos National Laboratory, an affirmative action/equal opportunity employer, is operated by the Los Alamos National Security, LLC for the National Nuclear Security Administration of the U.S. Department of Energy under contract DE-AC52-06NA25396. By acceptance of this article, the publisher recognizes that the U.S. Government retains a nonexclusive, royalty-free license to publish or reproduce the published form of this contribution, or to allow others to do so, for U.S. Government purposes. Los Alamos National Laboratory requests that the publisher identify this article as work performed under the auspices of the U.S. Department of Energy. Los Alamos National Laboratory strongly supports academic freedom and a researcher's right to publish; as an institution, however, the Laboratory does not endorse the viewpoint of a publication or guarantee its technical correctness.

## **Influence of Carbon Partitioning Kinetics on Final Austenite Fraction during Quenching and Partitioning**

A.J. Clarke<sup>1,2</sup>, J.G. Speer<sup>2</sup>, D.K. Matlock<sup>2</sup>, F.C. Rizzo<sup>3</sup>, D.V. Edmonds<sup>4</sup>, M.J. Santofimia<sup>5</sup>

<sup>1</sup>*Materials Science and Technology Division, Mail Stop G770, Los Alamos National Laboratory, Los Alamos, NM 87545, USA*

<sup>2</sup>*Advanced Steel Processing and Products Research Center, Colorado School of Mines, Golden, CO 80401, USA*

<sup>3</sup>*Department of Materials Science and Metallurgy, Pontifícia Universidade Católica-Rio de Janeiro, RJ 22543-900, Brazil*

<sup>4</sup>*School of Process, Environmental and Materials Engineering, University of Leeds, Leeds LS2 9JT, United Kingdom*

<sup>5</sup>*Instituto Madrileño de Estudios Avanzados en Materiales (IMDEA-Materiales), E. T. S. de Ingeniería de Caminos 28040 Madrid, Spain*

### **Abstract**

The quenching and partitioning (Q&P) process is a two-stage heat-treatment procedure proposed for producing steel microstructures that contain carbon-enriched retained austenite. In Q&P processing, austenite stabilization is accomplished by carbon partitioning from supersaturated martensite. A quench temperature selection methodology was developed to predict an optimum process quench temperature; extension of this methodology to include carbon partitioning kinetics is developed here. Final austenite fraction is less sensitive to quench temperature than previously predicted, in agreement with experimental results.

Keywords: quenching, partitioning, kinetics, austenite, martensite

The quenching and partitioning (Q&P) process was proposed [1,2] to create steel microstructures that contain martensite/austenite mixtures with tailored mechanical properties [2-6]. The Q&P process initially involves austenite formation, followed by quenching below the martensite start temperature  $M_s$  to obtain a specific fraction of martensite. A partitioning treatment follows the quenching step, with the aim of enriching the remaining untransformed austenite with carbon, by transport from the supersaturated martensite. The amount of final austenite may be modified upon quenching or cooling to room temperature, depending upon the austenite stability achieved during the partitioning treatment. The final desired microstructure consists of a mixture of carbon-enriched retained austenite and martensite (and perhaps intercritical ferrite), provided reactions competing with carbon partitioning can be suppressed.

A quench temperature selection methodology [2,7] was developed for the Q&P process that applies the Koistinen-Marburger [8,9] relationship to describe martensite formation to both the initial quenching step below  $M_s$  and the final quenching step to room temperature ( $\sim 25^\circ\text{C}$ ) after idealized, full partitioning. Idealized partitioning makes simplifying assumptions that all of the available carbon partitions to the austenite, that partitioning is complete (i.e. the kinetics of partitioning are ignored), and that no competing reactions occur, such as carbide precipitation or bainite formation. The results indicate an optimum quench temperature that yields a maximum amount of retained austenite. Above the optimum temperature, substantial austenite fractions

remain after the initial quenching step, but the austenite stability is too low during final quenching, and increasing amounts of fresh martensite form, reducing the final austenite fraction at room temperature. Below the optimum temperature, too much austenite is consumed during the initial quench prior to carbon partitioning, and the carbon content of the retained austenite is assumed to be greater than needed for stabilization at room temperature. The optimum is found at the particular quench temperature where martensite formation is just precluded during the final quench. Calculations made using this methodology guide the selection of quench temperatures needed to achieve substantial austenite fractions in experimental work [5]. From a Q&P alloy and process design perspective, the methodology developed has proved useful in predicting and understanding some important processing responses. However, this methodology does not incorporate partitioning kinetics or the associated carbon gradients developed within the austenite before the carbon partitioning process is complete.

In order to extend the methodology and begin to include partitioning kinetics, an approach is proposed that incorporates local carbon concentration profiles in austenite (and ferrite<sup>1</sup>) relative to the  $\alpha/\gamma$  interface as a function of partitioning time. The local austenite carbon concentration profile is then used to estimate austenite stability locally throughout the austenite, providing insight regarding final austenite fraction as a function of partitioning time for a given set of processing conditions. For these simulations, the ferrite was assumed to inherit the initial the parent austenite carbon content [10,11]. A cell of ferrite with a specific width, simulating a martensite lath, was adjacent to a cell of austenite with a specific width, simulating an austenite film; the  $\alpha/\gamma$  interface was assumed immobile [10,11]. Some simplifying assumptions about the microstructure scale, which controls the distance over which carbon diffusion occurs during idealized partitioning, were also made. Earlier work on lath width frequency distributions by Krauss and co-workers on 0.2 wt.% C martensite provided some guidance regarding appropriate martensite (ferrite) lath width dimensions [12,13]. The most frequently observed lath widths by Krauss and co-workers, determined from TEM replicas or thin foils, ranged approximately from 0.15 to 0.2  $\mu\text{m}$  [12,13]. Marder also reported that a lath width of 0.2  $\mu\text{m}$  was most frequently observed for 0.2 wt.% C martensite, regardless of austenitizing temperature over the range from 871-1204 °C [14]. A ferrite width of 0.2  $\mu\text{m}$  is therefore used here to represent typical (low carbon) lath martensite based on the work of Krauss and co-workers [12-14], although it is recognized that lath widths larger and smaller than 0.2  $\mu\text{m}$  are possible. For a given series of simulations, the ferrite width was assumed to be constant for a given quench temperature, while austenite film width varied according to the phase fractions.

Carbon profiles<sup>2</sup> from the center of a ferrite lath to the  $\alpha/\gamma$  interface and across the austenite half-film were predicted as a function of partitioning time and temperature using DICTRA software by Thermo-Calc [15]. The initial ferrite (martensite) was supersaturated with carbon from the parent austenite. As partitioning time increased, ferrite decarburization proceeded until 'complete' decarburization was achieved. The final carbon level in ferrite was slightly greater at higher partitioning temperatures due to the increased solubility of carbon in ferrite at elevated temperatures. Lower partitioning temperatures resulted in longer times for complete ferrite decarburization, as expected.

---

<sup>1</sup> Carbon concentration profiles were calculated for supersaturated ferrite, in order to simulate martensite. Differences between supersaturated ferrite and martensite (such as tetragonal lattice distortions), along with effects of carbon trapping by dislocations in martensite and carbide formation, were not incorporated.

<sup>2</sup> Ferrite or austenite half width dimensions were used in the simulations.

Short partitioning times were associated with significant austenite carbon enrichment near the interface. The levels of enrichment near the interface progressively decreased as partitioning time increased until a uniform carbon distribution was obtained across the entire austenite half width. The times for complete ferrite decarburization or austenite homogenization increased substantially as the scale of the microstructure increased.

Fractions of stable austenite across an austenite film were calculated “locally” from the austenite carbon concentration curves. The austenite stability calculations assumed that the Koistinen-Marburger equation [8,9] can be applied locally everywhere. For given quench and partitioning temperatures and at short times, only austenite present near the interface was predicted to be stable; austenite was not retained across the entire distance of the film, since steep carbon concentration gradients were predicted. The dependence of the total fraction of stable austenite (integrated over the film width) on partitioning conditions is influenced by the quenching temperature. Final austenite fraction as a function of quench temperature for a 0.19C-1.59Mn-1.63Si (wt.%) alloy is shown by the example solid curve in Figure 1 that assumes complete partitioning, calculated using the original quench temperature selection methodology that does not account for partitioning kinetics. Final austenite fractions calculated for the partitioning times examined (individual points) that incorporate partitioning kinetics at 400 °C are also shown in Figure 1. The final austenite fractions were calculated considering a ferrite half width of 0.1  $\mu\text{m}$  and austenite half widths ranging from  $\sim 7.5$  to  $\sim 72.5$  nm (depending upon quench temperature). Some interesting effects are observed that are further highlighted by the arrows in Figure 1, which indicate trends in austenite fraction with partitioning time.

As shown in Figure 1, below the optimum quench temperature of 240 °C (156 °C, for example) and accounting for the kinetics of carbon partitioning, the maximum amount of austenite is almost reached after partitioning for 0.01 s. Partitioning for 0.1 s is predicted to result in the maximum austenite amount, and partitioning for longer times results in this same value. Thus, the left arrow in Figure 1 qualitatively shows the austenite amount increasing monotonically up to  $\sim 7$  vol.% as partitioning time increases. Above the optimum quench temperature of 240 °C (319 °C, for example) and accounting for partitioning kinetics, the maximum amount of austenite is achieved after partitioning for 0.1 s. This austenite amount is greater than predicted by the curve. Increases in partitioning time beyond 0.1 s result in a *decreasing* austenite fraction toward the value given by the solid curve, which was predicted using the original quench temperature selection methodology. Specifically, the amount of austenite increases initially up to  $\sim 9$  vol.% and then decreases with increasing partitioning time until the curve is eventually reached at long times. This behavior is indicated by the right arrows in Figure 1, which apply to quench temperatures above the optimum.

It is interesting to note that the final austenite fraction is somewhat insensitive to quench temperature in Figure 1 for many of the partitioning times considered, in contrast to the sharp maximum at the endpoint of partitioning predicted by the original methodology. These behaviors might have important implications with respect to industrial processing, suggesting the possibility of an expanded processing window where the effect of quench temperature on austenite fraction may be less sensitive than initially suspected.

Figure 2 shows *experimentally measured* austenite fractions plotted versus quench temperature for a 0.19C-1.59Mn-1.63Si (wt.%) steel processed via Q&P. (Note that intercritical annealing was performed, whereas the results in Figure 1 assume full austenitization prior to Q&P.) The arrows highlight trends with partitioning time for each quench temperature examined. Figure 2 also contains the final austenite fraction curve after full partitioning, calculated using the original

quench temperature selection methodology (i.e. ignoring kinetics). Consistent with the behavior predicted in Figure 1, greater austenite fractions than predicted by the final austenite fraction curve are measured for quench temperatures above the optimum quench temperature of 240 °C (260 °C, for example). Austenite fractions above the predicted curve were also indicated in recent experimental results obtained by De Moor *et al.* for a single partitioning time [3]. For quench temperatures below 240 °C, the maximum austenite fraction is obtained experimentally after partitioning for 10 s at 200 °C. Increasing partitioning time results in decreasing austenite fraction, which is different from the behavior predicted for low quench temperatures in Figure 1. Competing reactions are ignored in the calculations used to generate the predictions in Figure 1, and carbide formation has been suggested to explain an eventual decrease in experimental austenite fraction with increasing partitioning time [5,16,17]. Although some of the austenite fraction trends predicted in Figure 1 appear to agree qualitatively with the limited experimental results available and shown in Figure 2, additional investigations regarding the influence of quench temperature on final austenite fraction during Q&P are needed to understand better and confirm the predicted trends.

Additionally, the partitioning times predicted to maximize austenite amount (Figure 1) are short compared to the times examined in the experimental work (Figure 2). Simulations were also performed for a ferrite half width of 1 $\mu$ m to explore the influence of microstructure scale on the partitioning kinetics. Although the results are not shown here, the time predicted to reach the maximum austenite fractions shown in Figure 1 for the quench temperatures 156 and 319 °C was approximately 10 s, in better agreement with the times used in the experimental work.

In conclusion, the quench temperature selection methodology that predicts retained austenite fractions after Q&P processing was extended to include the kinetics of carbon partitioning. Aspects of the predicted austenite fraction trends as a function of quench temperature agree with some of the trends obtained from experimental work. Importantly, the results also suggest that an expanded processing window may be available, due to reduced quench temperature sensitivity than is indicated from a methodology based on the assumption of full carbon partitioning.

### Acknowledgements

The authors gratefully acknowledge the support of the Advanced Steel Processing and Products Research Center, a National Science Foundation Industry/University Cooperative Research Center, at the Colorado School of Mines and the Inter-American Materials Collaboration Program. Funding is acknowledged from NSF award #0303510 (USA), CNPq (Brazil) and EPSRC (United Kingdom). The authors also thank POSCO for providing the experimental material. Technical assistance and helpful discussions provided by K.D. Clarke, E.J. Pavlina, and E. De Moor are also greatly acknowledged; the helpfulness of A.R. Martins is also greatly appreciated.

### References

- [1] J.G. Speer, D.K. Matlock, B.C. DeCooman, J.G. Schroth. *Acta Mater*, 2003; 51:2611.
- [2] J.G. Speer, D.V. Edmonds, F.C. Rizzo, D.K. Matlock. *Curr Opin Solid State Mater*, 2004; 8:219.
- [3] E. De Moor, S. Lacroix, A.J. Clarke, J. Penning, and J.G. Speer. *Metall Mater Trans A*, 2008; 39A:2586.
- [4] E. De Moor, C. Föjer, A.J. Clarke, J. Penning, and J.G. Speer. In: T. Perez, editor. *Proceedings, New Developments on Metallurgy and Applications of High Strength Steels*,

- Buenos Aires (Argentina): Tenaris, Ternium, and Argentina Association of Materials, 2008, Paper #2, 9 pages. And, In: T. Perez, editor. Proceedings of the Conference on New Developments on Metallurgy and Applications of High Strength Steels, Warrendale (PA): TMS, 2009, p.721.
- [5] A. Clarke. Ph.D. Thesis, Golden (CO): Colorado School of Mines, 2006.
- [6] A.M. Streicher, J.G. Speer, D.K. Matlock, and B.C. DeCooman. In: J.G. Speer, editor. International Conference on Advanced High-Strength Sheet Steels for Automotive Applications Proceedings, Warrendale (PA): AIST, 2004, pp.51-62.
- [7] J.G. Speer, A.M. Streicher, D.K. Matlock, F.C. Rizzo, and G. Krauss. In: E.B. Damm and M. Merwin, Austenite Formation and Decomposition, Warrendale (PA): ISS/TMS, 2003, pp. 505-522.
- [8] D.P. Koistinen and R.E. Marburger. *Acta Metall*, 1959; 7:59.
- [9] G. Krauss. *STEELS: Heat Treatment and Processing Principles*, Metals Park (OH): ASM International, 1990.
- [10] M. Hillert, L. Höglund, J. Ågren. *Acta Metall Mater*, 1993; 41(7):1951.
- [11] DICTRA Examples, Version 23, Stockholm (Sweden): Thermo-Calc Software AB, 2004, pp. 231-244.
- [12] C.A. Apple, R.N. Caron, and G. Krauss. *Metallurgical Transactions*, 1974; 5:593.
- [13] T. Swarr and G. Krauss. *Metall Trans A*, 1976; 7A:41.
- [14] A.R. Marder. Ph.D. Thesis, Bethlehem (PA): Lehigh University, 1968.
- [15] Thermo-calc Software, <http://www.thermocalc.com/>
- [16] A. Clarke, J.G. Speer, D.K. Matlock, F.C. Rizzo, D.V. Edmonds, and K. He. In: J.M. Howe, D.E. Laughlin, J.K. Lee, U. Dahmen, and W.A. Soffa, *Solid-Solid Phase Transformations in Inorganic Materials 2005 Volume 2*, Warrendale (PA): TMS, 2005, pp. 99-108.
- [17] A.J. Clarke, J.G. Speer, M.K. Miller, R.E. Hackenberg, D.V. Edmonds, D.K. Matlock, F.C. Rizzo, K.D. Clarke, and E. De Moor. *Acta Mater*, 2008; 56:16.

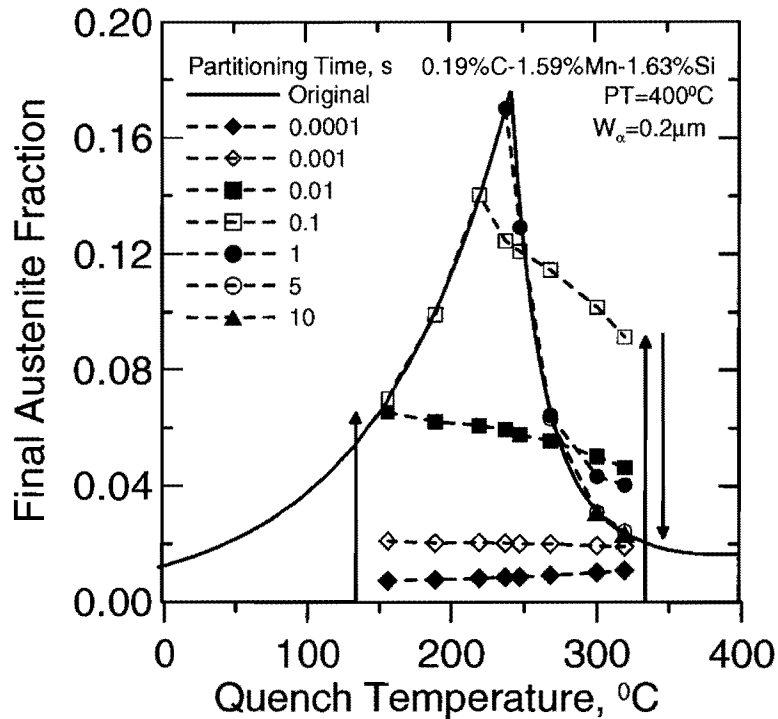


Figure 1: Calculated final austenite fraction as a function of quench temperature for a 0.19C-1.59Mn-1.63Si (wt.%) alloy. A final austenite fraction curve (solid curve) is shown that does not incorporate carbon partitioning kinetics. (The solid curve was produced using the original quench temperature selection methodology [2,7].) Individual points that incorporate the kinetics of carbon partitioning are also shown for select partitioning times. A constant ferrite half width of 0.1  $\mu\text{m}$  was used for the partitioning temperature 400 °C. Arrows highlight austenite fraction behaviors with increasing partitioning time for quench temperatures above and below the optimum quench temperature.

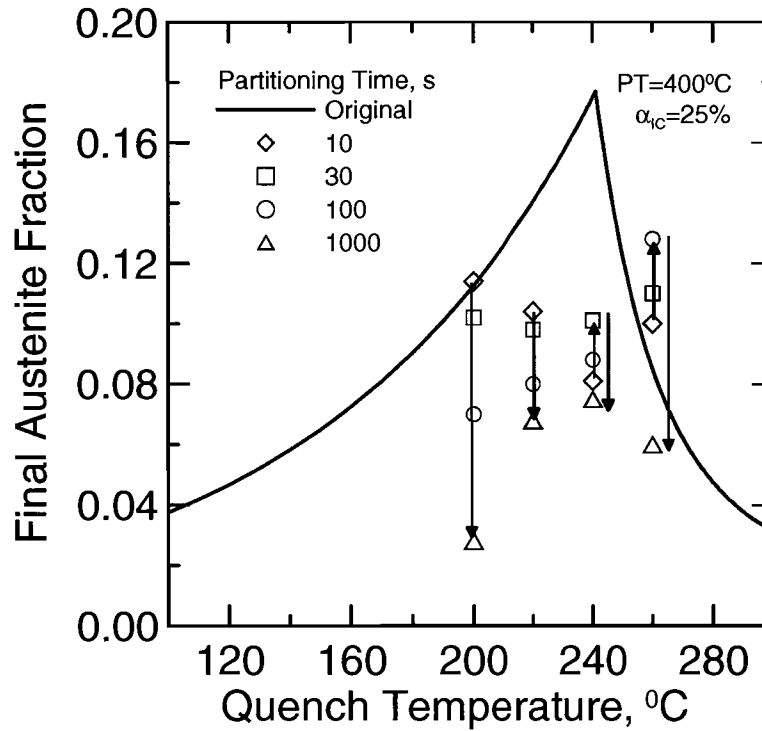


Figure 2: Experimental final austenite fractions for a 0.19C-1.59Mn-1.63Si (wt.%) steel as a function of quench temperature for different partitioning times for samples intercritically annealed at 820 °C for 180 s, quenched to 200, 220, 240, or 260 °C for 10 s, partitioned for 10, 30, 100, or 1000 s at 400 °C, and then water quenched to room temperature. Arrows highlight the behaviors exhibited as a function of partitioning time. A final austenite fraction curve (solid curve) is also shown that was calculated using the original quench temperature selection methodology [2,7].